TECHNICAL DESCRIPTION AND STATUS OF THE EMMA NON-SCALING FFAG

N.Bliss, C.D.Beard, J.A.Clarke, S.A.Griffiths, N.Marks, P.A.McIntosh, B.D.Muratori, B.J.A.Shepherd, S.L.Smith, S.I.Tzenov, STFC Daresbury Laboratory, Warrington, UK.

T.R.Edgecock, D.Kelliher, S.Machida, STFC Rutherford Appleton Laboratory, Didcot,UK

Abstract

EMMA, the worlds first non-scaling fixed field alternating gradient (ns-FFAG) accelerator, is to be constructed at STFC Daresbury Laboratory as part of the BASROC consortium's CONFORM project. EMMA, a 10 to 20 MeV electron ring, will demonstrate the principle of ns-FFAGs and be used to study and understand the features of this novel type of acceleration. The knowledge gained will inform the design of PAMELA, a machine for medical research, and a range of potential applications being studied. EMMA is being designed by an international collaboration and funded by the UK 'Basic Technology' initiative. The current status of this project is presented including the technical description of the key hardware implemented during the design phase of the project.

INTRODUCTION

The British Accelerator Science and Radiation Oncology Consortium (BASROC) is an association of specialists in the fields of accelerator science, particle physics, engineering, medical physics and medicine with the aim of developing the next generation of accelerators for science, medicine and industry [1].

BASROC has been successful in gaining funds for its 1st project from the UK's Technology Research Programme, a scheme that crosses the different funding agencies to "contribute to the development of a generic technology base that can be adapted to a diverse range of scientific research problems and challenges" [2].

The project has been named the Construction Of an Non-scaling FFAG For Oncology, Radiation and Medicine, CONFORM [3]. The funding is £8m over a 3.5 year period and started in April 2007. The project has 3 related work packages that are being delivered simultaneously:

- Electron Model for Many Applications (EMMA), which is a design, construction and commissioning project.
- Particle Accelerator for MedicaL Applications (PAMELA), which is a design study.
- Applications, which is also a study of the wide ranging potential exploitation of the ns-FFAG.

The ns-FFAG method of acceleration [4] and the EMMA machine concept [5] have existed for a number of years. As well as proving the principle of ns-FFAGs, EMMA will bring a detailed understanding of the features of this type of accelerator, information which will be of benefit to the varied applications being considered.

EMMA is being designed by an international collaboration involving: BNL, CERN, FNAL, LPSC, TRIUMF and the UK's accelerator science centres - The Cockcroft Institute and the John Adams Institute. The design is well advanced and the technical description will form the main content of this paper. EMMA is the major work package of the CONFORM project in terms of cost at £5.6m and will be constructed at the Science and Technology Facilities Council, Daresbury Laboratory site, using the Daresbury Energy Recovery Linac Prototype as the injector [6].

AIMS AND REQUIREMENTS OF EMMA

The diverse range of applications demands high power beams, at reasonable cost and with good reliability. FFAG rings offer a radical alternative to conventional accelerator technologies as they can deliver these requirements simultaneously. With fixed magnetic fields, like a cyclotron, and strong focussing, like a synchrotron, they combine many of the positive features of both. In particular FFAGs have:

- Fixed magnetic fields, enabling FFAGs to be cycled more quickly than synchrotrons. This also leads to simpler and cheaper power supplies and makes an FFAG easier to operate than a synchrotron.
- Higher beam acceptance, giving high intensities at low beam loss, so that operation and maintenance are easier, safer, and more cost effective.
- A magnetic ring, like a synchrotron, reducing cost relative to a cyclotron, while allowing beam extraction at any energy.
- Higher energy, since the beam can be accelerated in a series of rings, enabling acceleration of ions.
- Compact size, making them easier to locate in industrial and clinical environments.

What distinguishes an FFAG from a cyclotron is that alternating gradient focusing is employed to reduce the magnet aperture, at the cost of having to keep the RF synchronised with the beam as it is accelerated. All FFAGs which accelerate the beam must contend with this time of flight variation.

The ns-FFAG was invented in 1999 [4]. The magnetic design gives a parabolic variation of orbit length with energy [7], which can be arranged to greatly compress the range of orbit radii, and thus the magnet aperture, as a function of energy, while maintaining a linear magnetic field dependence. The small apertures and linear fields

allow simplification and cost reduction compared with the scaling FFAGs. A further advantage is that for certain applications it is possible to use fixed-frequency RF, allowing continuous operation like a cyclotron.

EMMA will be the first ns-FFAG ever constructed and although the theory and simulations have been well tested for muon applications, the new ring will demonstrate that particles can be accelerated with the non-scaling method and also study beam dynamics [8,9]. Two broad issues will be studied in particular:

- Resonances.
- longitudinal dynamics.

Scaling FFAGs have tunes which are independent of energy. This allows one to choose a working point away from the important resonances and stay there throughout the acceleration cycle. A ns-FFAG has a tune which varies with energy. Thus, the beam will pass through a number of resonances during the acceleration cycle. Normally, this would lead to unacceptable beam loss. In the ns-FFAG this is mitigated by several factors:

- The lattice consisting of entirely short, identical cells with minimum magnet errors.
- Linear magnets (for muon and electron acceleration) - thus the non-linear resonances are only weakly driven.
- Rapid acceleration - complete in as little as 16 turns, consequently the passage through the resonance is fast, and successive perturbations should not have the opportunity to add coherently to a dangerous level.

The disadvantage of using an FFAG over a cyclotron is that the time of flight depends on energy. Thus, if one has fixed frequency RF, and one accelerates over too large a range, the bunches will eventually drift out of phase with the RF. There are a number of ways to deal with this, but the method chosen for EMMA is to accelerate only over a factor of 2 in momentum. This generally means the acceleration will be completed in less than 20 turns. The dynamics in the longitudinal phase space for this time of flight is unique and a machine has never been operated in this mode. Therefore, to explore these dynamics in detail, there is a requirement to modify the parameters that govern the acceleration mode:

- amount of RF voltage.
- RF frequency.
- behaviour of time of flight as a function of energy.

A major aim will be to verify that the predictions of theoretical models are correct.

EMMA must also be capable of:

- variable acceleration rate.
- acceleration by a factor of 2 in momentum.
- injection and extraction at all energies.

EMMA PARAMETERS

EMMA is similar in design to a muon accelerator FFAG. The parameters, shown in Table 1, are based on those designs and suitably scaled. Electrons are used to reduce costs to an acceptable level. Figure 1 shows the EMMA layout in the ERLP accelerator hall.

Table 1: Basic Parameters

Energy range	10 – 20 MeV
Lattice	F/D Doublet
Circumference	16568.202 mm
No of cells	42
Normalised transverse acceptance	3 mm
Frequency (nominal)	1.3 GHz
No of RF cavities	19
Average beam current	13 μA
Repetition rate	1, 5, 20 Hz
Bunch charge	16-32 pC single bunch

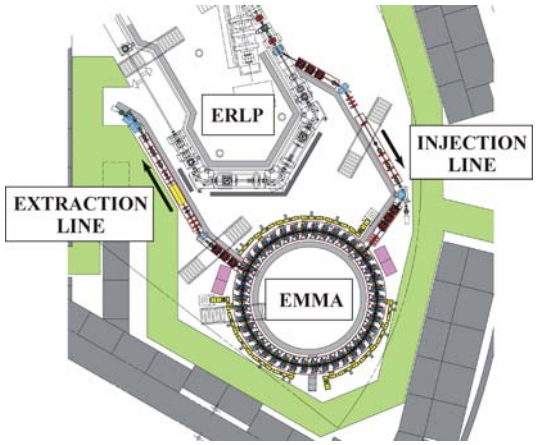

Figure 1: EMMA in the ERLP accelerator hall.

HARDWARE INTEGRATION

The EMMA lattice has been studied in detail and the reasoning behind the configuration described [9]. A doublet lattice chosen with 42 cells is an appropriate model at affordable cost. A sectional model through two cells is shown in Figure 2 that repeats around the circumference of the EMMA ring.

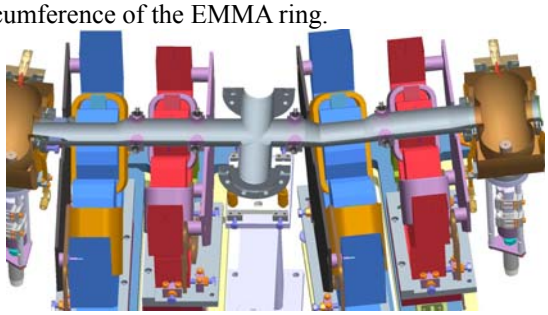

Figure 2: Section through two EMMA cells.

The magnets need to be combined function. However, in practice, the dipole component in EMMA is found to

be much smaller than the quadrupole. As a result, they are being implemented as alternately horizontally focusing and defocusing quadrupole magnets. The geometry is described in Table 2.

Table 2: Cell Geometry

Long drift length for the RF cavity, diagnostic or pumping	210.000 mm
F magnet nominal field length	58.782 mm
Short drift length	50 mm
D magnet nominal field length	75.699 mm
Cell length	394.481 mm

The dipole component is obtained by positioning the magnets off centre. Independent variable control of these components is achieved by varying the quadrupole strength and independently adjusting the magnet offset. Consequently, all 84 quadrupoles are mounted on motorised precision linear slides with 1 μm repeatability.

19 RF cavities fit in the long drift length in every other cell, accept in the regions of injection and extraction. Cells not containing cavities will accommodate vacuum pumping, diagnostic devices and vertical correctors. 84 beam position monitors 2 per cell are integrated close to the magnets, but sufficiently far from the high voltage generated in the vacuum chamber from RF cavities.

Studies have shown that the quadrupole doublet and the RF cavity in each cell can be aligned parallel without any significant reduction in performance. This will simplify the engineering construction and reduce cost.

To ensure that the quadrupole magnet fields are as identical as possible in all cells, field clamp plates are required at the entrance and exit of each doublet.

The space volume defined makes it very challenging to accommodate all the necessary devices to meet the aims for EMMA, particularly at the regions of injection and extraction. Figure 3 shows the injection area, where a septum, kicker, kicker configuration is utilised to inject the beam into EMMA [10]. A similar kicker, kicker, septum configuration is utilised for extraction. The design of the septum, kickers and fast pulsed power supplies is in progress.

Figure 3: Injection region showing the kicker, kicker, septum configuration.

A feature of the ns-FFAG is relatively small beam apertures, which results in an acceptable internal circular aperture of diameter 40 mm in the RF cavity and D quadrupole. A larger aperture of diameter 48 mm is required in the F quadrupole. Lateral offsets in the magnet position and the requirement to translate the magnets results in larger magnet apertures, F quadrupole R37 mm and D quadrupole R 53 mm.

To save space by minimising the quantity of vacuum flanges a common standard vacuum chamber covering 2 cells has been adopted in general, with special chambers in the injection and extraction regions. An integral single flexible bellows in every 2 cells accommodates thermal expansion, while also providing the flexibility to make the vacuum joints.

EMMA RING QUADRUPOLE MAGNETS

Due to the relatively large magnet inscribed radii compared to the short magnetic length requirement, each magnet has a rather unusual aspect ratio - the yoke thickness being of the same order as the inscribed radii. The field is therefore dominated by end effects [11], which in conventional storage ring magnets are small corrections.

In an FFAG, the beam moves significantly inside the vacuum chamber as it is ramped in energy. The required horizontal aperture is therefore rather large, and consequently the good field region specified for the magnets is quite demanding.

Interaction between the two magnets in a cell must be taken into consideration, as well as fields in the straight sections.

Full 3D modelling using CST EM Studio [12] has been employed from the outset, and the results have been cross-checked with OPERA-3D [13]. A pair of prototype magnets is being built by Tesla Engineering [14], to verify the simulation work.

Magnet Parameters

Table 3: Magnet parameters

Parameter	**F magnet**	**D magnet**	**Units**
Integrated gradient	-0.387	0.347	T
Inscribed radius	37	53	mm
Current	213.4	263.5	A
Turns in coil	11	11	
Yoke thickness	55	65	mm
Pole width	73	100	mm
Horizontal movement range	-2.711 +2.604	-5.28 +14.535	mm
Offset from magnetic centre	7.507	34.025	mm
Required good field region	-32…+16	-56…-10	mm

Magnet Modelling

Each magnet was optimised separately in EM Studio, with a view to tweaking the combined model at a later stage and providing a field map to use in tracking studies, iterating the design further. The goal was to achieve as large a possible region within which the integrated

gradient variation did not exceed ±0.1%. The design goals were specified as ±32mm for the F magnet and ±56mm for the D magnet. These apertures are defined by the required beam movement as the energy changes, plus the horizontal movement specified for each magnet.

Initially, two variables were used in the simulation – tangent point and the size of the chamfer at the pole ends. For a normal (long) storage ring quadrupole, this would give sufficient degrees of freedom – adjusting the tangent point to correct the central field, and then adding a chamfer to correct for end effects. However, in these very short magnets, the end fields dominate the overall field quality, and the gradient map seems to have features which cannot be corrected for using these variables alone. The maximum good field region for the F magnet available using this geometry (including a field clamp) was ±14mm.

A new approach was tried, changing from the old pole face model that used a hyperbolic section and a tangent section.

'Straight-Line' Pole Geometry

An arbitrary pole design provides the freedom to adjust the field profile with fewer restraints than that imposed by a 'traditional' quadrupole design. However, it raises the question of how to parameterise the pole. The model initially tried was based on the following steps (see Figure 4 for definition of parameters):

- Begin with a square pole.
- Remove material from each side of the pole, adjusting the d_0 point until reaching an optimum.
- Adjust the d_1 point, halfway between the pole centre and the side.
- Introduce a third (d_2) point halfway between the two previous points, and adjust this.

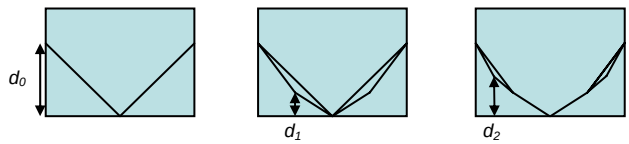

Figure 4: Optimisation of straight-line geometry for an even number of pole tip facets. Points are introduced one at a time, optimising at each step.

This method turns out to be very successful in generating a pole geometry that conforms to the specification. With no field clamps, the F good field region was extended to ±32mm. Adding the field clamp, however, has an adverse effect on the field quality.

The shape of the vacuum window in the field clamp was altered to try to improve the field quality. The optimum shape was found to be one following the outline of the magnet poles. This has the advantage of keeping the quadrupole symmetry, so that field quality in the vertical direction does not require further evaluation.

A variant of the straight-line pole tip geometry was tried in which an odd number of pole tip faces were used. Designs with three and five faces, using one and two variables respectively, were tried out (Figure 5). The optimisation was done sequentially as above, based on the assumption that the two variables were fairly orthogonal.

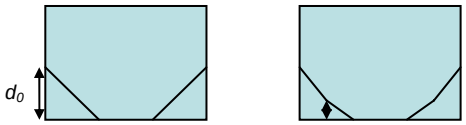

Figure 5: Optimisation of straight-line geometry for an odd number of pole tip facets (three and five).

For the F magnet, the best result was found for a five-face geometry with d_0 = 19.5mm and d_1 = 4.25mm, resulting in a good field region of ±22.9mm (Figure 6). This is somewhat short of the specified value of 32mm. It may become clearer whether this could be acceptable or not when tracking studies are carried out using real simulated field maps from this study.

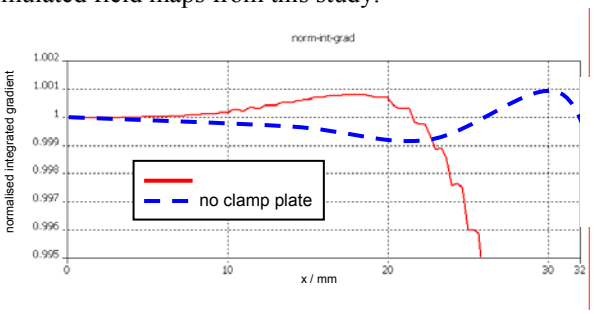

Figure 6: Normalised integrated gradient plot of the optimum configuration for the F magnet. The good field region is 22.9mm. A plot for a magnet with no clamp plate is also shown.

Similar results were obtained for the D magnet, and an optimum pole shape was found which resulted in a good field region of ±32mm.

Prototype Magnets

Since these are rather unusual magnets, a pair of prototypes have been built to confirm the results from computer modelling. These will be complete in September 2007, and will be tested using rotating coil and Hall probe methods to ensure they meet the specifications.

Further Magnet Work

A field map of the entire cell has been generated and will be used in the FFEMMAG code to track a beam around the entire machine. Optimisation of the magnet design will continue in parallel with procurement of the production magnets.

The field clamp was introduced primarily to reduce stray fields in the kicker straights. Once some detailed kicker modelling has been carried out, it may be possible to modify the field clamp geometry, and try to improve the field quality in the quadrupoles.

RADIO FREQUENCY SYSTEM

To provide the necessary acceleration to the electrons a suitable RF system is being developed. Due to the compact nature of the accelerator there are demanding boundary conditions that the system has to adhere to.

In order to understand the full system a cavity design had to be provided to deliver the RF power requirements. A suitable RF power source has been identified, and subsequently a digital control system is being developed to ensure that the correct amplitude and phase is delivered to each cavity during operation.

As a result of this process, different parts of the RF system are at varying levels of progression, and therefore not yet fixed.

RF Cavity

In order to synchronise with the injector RF system, a 1.3 GHz frequency was proposed. The cavity design was heavily influenced by geometrical restrictions. The longitudinal space for the cavity is confined to 110 mm including flanges. Also due to the beam orbit variation the cavity beam pipe aperture had to be a minimum of 40 mm diameter. As a result of this, a less than optimal cavity efficiency is achieved than for an unrestricted cavity design. Optimisation of the cavity shape was carried out to maximise the shunt impedance to reduce the RF power needed.

Maximum shunt impedance was obtained by adopting a normal conducting, single cell and re-entrant cavity design. Coupling into the cavity and frequency tuning is provided by means of a coupling loop and capacitive post respectively.

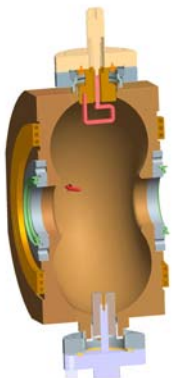

Figure 7: RF cavity.

The final design calculations indicate a shunt impedance of 4.3 MΩ, however, once the device is constructed, a more realistic value of 80% (3.4 MΩ) is assumed, due to wall losses and apertures. In order to provide the minimum required acceleration of 120 kV per cavity, over 2 kW per cavity will be required. It is anticipated that the total acceleration per turn could increase as high as 180 kV per cavity, requiring a maximum of 6.1 kW per cavity. The final parameters for the cavity design are summarised in Table 4. Finite element analysis of the thermal and structural behaviour is complete and predicts less than 20μm deformation of the nose cone gap with the input power averaged at 200W. A prototype cavity construction programme is now in progress.

Table 4: Final Cavity Design Parameters

Parameter	**Value**	
Frequency	1.3 GHz	
Theoretical Shunt Impedance	4.3 MΩ	
Realistic Shunt Impedance (80%)	3.44 MΩ	
Qo	23,000	
R/Q	120 Ω	
Tuning Range	+1.5 to -4 MHz	
Accelerating Voltage	120 kV	180 kV
Power (kW)	2.1 kW	4.7 kW
P_{total} including 30% overhead	2.7 kW	6.1 kW

Power Source and Distribution

In order to deliver 2.7 kW per cavity, with the potential of increasing by a further 3.4 kW, the system needs to overcome parasitic losses in the RF distribution system and also cope with LLRF and HPRF stability effects. These have been estimated as an additional 30 % RF power requirement.

Two alternatives being considered are a high power Klystron, capable of delivering 160 kW with a split distribution to all 19 cavities, or 3 IOTs each powering 6 or 7 cavities each. A power supply unit already exists at Daresbury with a large enough capacity to run both options.

Each option has its own benefits: IOTs are more compact and cheaper devices that can be replaced promptly in the event of a failure, but this system will require extensive reconfiguration of the PSU. The Klystron offers a much larger overhead in the event of operating at higher energies, however the cost and likelihood for replacement make this a very risky alternative. Table 5 outlines the options.

Table 5: RF power delivery options

	160 kW Klystron	30 kW IOT	Units
No. of Cavities	19	19	
No. of Power Sources	1	3	
R_{sh}	3.4	3.4	MΩ
V_{acc}/Cavity	120 (180)	120 (180)	kV
Cavities/source	19	2x6/1x7	
RF Power/Cavity (including overhead)	2.73 (6.1)	2.73 (6.1)	kW
Distribution and Control Overhead	40	40	%
Total Ring RF Power	51.3 (115.9)	51.3 (115.9)	kW
Max Ring Power Available	160	90	kW
RF Power Overhead	108.7 (44.1)	44.1 (-25.9)	kW

For both options a number of cavities are going to be powered from a single source, therefore to minimise the size of the waveguide distribution the cavities are placed in series (or cascaded) instead of a parallel technique using a number of hybrid splitters.

For the cascaded system, each cavity will require a load, hybrid splitter and individual 3 stub tuner to allow adjustment of RF phase during operation. In order to ensure the same power is delivered to each cavity a series of hybrids with increasing coupling along the circuit until finally the power is split equally between the last two cavities in the line. A schematic of the waveguide components required per cavity can be seen in Figure 8.

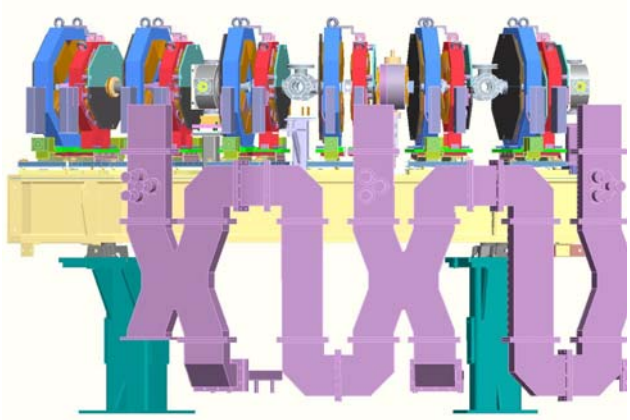

Figure 8: RF waveguide cascaded distribution.

This scheme highlights the size of the components required per cavity in relation to the size of the cavity. Operating a number of cavities from a single source introduces further difficulties with the LLRF controls system. For both options however, a LLRF controls system is currently being designed to provide sufficient amplitude and phase control for operations.

DIAGNOSTICS

As EMMA is an experimental machine, having sufficient diagnostics is crucial. Work is in progress on the specification, design, quantity and location of the devices. The current requirements and how they will be met are summarised in Table 6.

Table 6: The diagnostics requirements of EMMA.

Measurement	Device	Number
Injection Line		
Beam position	4 button BPM	**5**
Beam profile	Screen & wire scanner	1 1
Beam current & phase wrt RF	Resistive wall monitor	1
Emittance	Screen	3
Momentum	Spectrometer	1
Transmission	Faraday cup	1
Ring		
Beam position	4 button BPM	84
Beam profile	Screen & wire scanner	2 2
Beam current & phase wrt RF	Resistive wall monitor	1
Beam loss	Beam loss monitor	4 sectors
Extraction Line		
Beam position	4 button BPM	**5**
Beam profile	Screen & wire scanner	1 1
Beam current & phase wrt RF	Resistive wall monitor	1
Emittance	Screen	3
Momentum	Spectrometer	1
Long. Profile	Transverse deflecting cavity and screen	1
Transmission	Faraday cup	1

REFERENCES

[1] BASROC: http://www.basroc.org.uk

[2] R.J.Barlow et al, "The CONFORM Project: Construction of a Non-Scaling FFAG and its Applications", PAC'07, Albuquerque, 2007

[3] CONFORM: http://www.conform.ac.uk

[4] C. Johnstone et al, "Fixed Field Circular Accelerator Designs", PAC'99, New York, March 1999, p. 3068.

[5] S. Koscielniak et al. "Report of Working Group I: FFAG for Muon Physics", Proc. of the International Workshop on FFAG Accelerators, FFAG04, Tsukuba, Japan, 2004, page 27.

[6] S.L.Smith et al, "The Status of the Daresbury Energy Recovery Linac Prototype", PAC'07, Albuquerque, 2007.

[7] C. Johnstone and S. Koscielniak, "Longitudinal Dynamics in an FFAG Accelerator under Conditions of Rapid Acceleration and Fixed, High RF", PAC'03, Portland, May 2003, p. 1831.

[8] R. Edgecock "EMMA – the World's First Non-scaling FFAG", PAC'07, Albuquerque, 2007.

[9] J.S.Berg et al, "The EMMA Lattice Design", PAC'07, Albuquerque, 2007.

[10] T. Yokoi, "Beam Injection and Extraction in EMMA NS-FFAG Ring", PAC'07, Albuquerque, 2007.

[11] B. Shepherd and N. Marks "Quadrupole Magnets for the 20 MeV FFAG, 'EMMA'", PAC'07, Albuquerque, 2007.

[12] CST simulation software, http://www.cst.com

[13] OPERA magnet modelling software, http://www.vectorfields.com.

[14] Tesla Engineering, http://www.tesla.co.uk.